

**COMPARISON BETWEEN PHENOMENOLOGICAL AND EMPIRICAL MODELS FOR
POLYMERIZATION PROCESSES CONTROL****Tiago F. Finkler¹, Gustavo A. Neumann², Nilo S. M. Cardozo³, Argimiro R. Secchi⁴***1,3,4 – Grupo de Modelagem, Simulação, Controle e Otimização de Processos (GIMSCOP)
Departamento de Engenharia Química – Universidade Federal do Rio Grande do Sul**Rua Sarmento Leite, 288/24 – CEP: 90050-170 – Porto Alegre – RS – Brazil**Phone: +55-51-3316-3528 – Fax: +55-51-3316-3277**2- Braskem S/A, III Pólo Petroquímico, Via Oeste, Lote 5 – CEP: 95853-000 – Triunfo – RS – Brazil**Phone: +55-51-457-5495 – Fax: +55-51-457-5450**E-mail: {¹tiago, ³nilo, ⁴arge}@enq.ufrgs.br, ²gustavo.neumann@braskem.com.br*

Abstract: In this work, linear, quadratic, and nonlinear empirical models were built and compared with a dynamic nonlinear phenomenological model with respect to the capability of predicting the melt index and polymer yield rate of a low density polyethylene production process. Based on steady-state gains and on known first and second order time constants of the process, the empirical models were generated using PLS, QPLS, and BTPLS methods in order to predict the system dynamics. As the quadratic model provided more reliable predictions, it was used as melt index virtual analyzer of an advanced control strategy for an industrial plant, improving the controller action and the polymer quality by reducing significantly the process variability.
Copyright © 2006 IFAC.

Keywords: partial least squares, empirical modelling, parameter estimation, phenomenological modelling, LLDPE.

1. INTRODUCTION

Correctly validated multivariate models are useful tools for the development of reliable predictive controllers in polymerization processes.

Depending on their nature, empirical or phenomenological, these models may provide different levels of information about the process. When those kinds of models are compared, phenomenological models are supposed to show higher extrapolation capability. However, empirical models require much less investments in modelling, especially when little is known about the physical and chemical phenomena underlying the process.

Concerning specifically to the modelling of polyolefin polymerization processes, many studies have been developed in the last decades. Sato et al

(2000) studied the modelling and simulation of an industrial gas-phase ethylene polymerization process, based on the phenomenological model of McAuley (1991), for using in nonlinear controller design for melt index and density. Many published papers deal with modelling and parameter estimation for nonlinear model predictive controller design in industrial applications, like Zhao (2001) and Soroush (1998). Bindlish et al. (2003) studied the parameter estimation problem for industrial polymerization processes. In their work, two kinetic parameters were estimated for Exxon's homo and copolymerization to use in monitoring and feedback control systems of these processes.

In this work phenomenological and empirical models for the prediction of yield and melt index of an industrial process for the production of linear low-

density polyethylene (LLDPE) are compared. The studied process is composed by two gas-phase reactors connected in series. For both reactors, the considered operational variables (model inputs) are the ethylene (C2), butene (C4) and hydrogen (H2) concentrations, catalyst flow rate (Cat), the bed temperature (T), total pressure (P), and fluidized bed level (L). The response variables (model outputs) are the polymer melt index (MI) and polymer yield rate (YR) at the outlet of each reactor. The studied process is schematized in Figure 1:

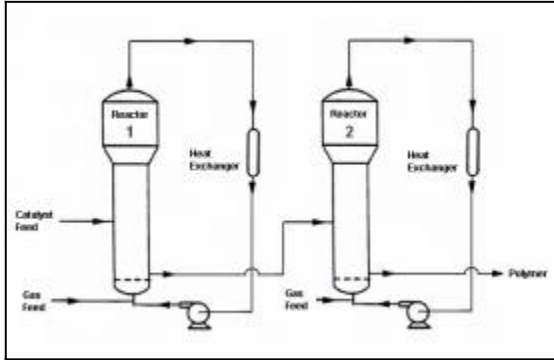


Figure 1: Scheme of the polymerization process.

Two ten-days dataset containing measurements of all considered variables were collected. The sampling rate varies from one variable to another. For the variables measured on line (T, P, C2, C4, H2 and Cat) it is in the order of minutes while for MI it is in the order of hours. In this text, the first dataset will be treated as dataset A and the second dataset will be treated as dataset B. These data sets are presented in Figure 2 and in Figure 3. The vertical axis of the plots correspond to the coded variables measurements and the horizontal axis correspond to the time window where these variables measurements were made.

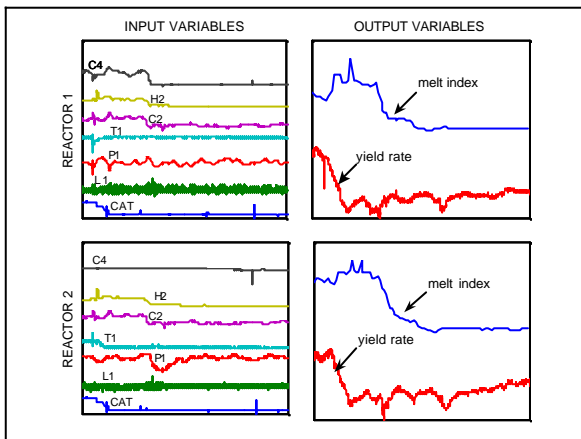


Figure 2: Process first dynamics dataset (A).

2. PHENOMENOLOGICAL MODEL

Industrial fluidized-bed reactors have been modelled by several authors, see for example Kunii and Levenspiel (1991) and Choi and Ray (1985). According to the model proposed by Gambetta et al. (2001), the fluidized bed can be divided in two regions: an emulsion phase and a bubble phase,

connected by heat and mass transfer between them. The emulsion phase has a solid phase (polymer and catalyst), a gas phase at the minimal fluidization condition, and a gas phase adsorbed by the solid phase. The bubble phase is composed by the excess of gas required to keep the emulsion phase at the minimal fluidization condition. In the disengagement section, it is only considered the gas phase.

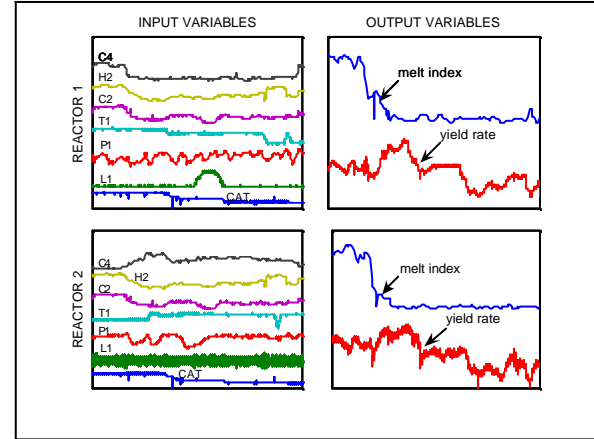


Figure 3: Process second dynamics dataset (B).

The kinetic model was developed for Ziegler-Natta catalysts, considering the following reactions: spontaneous activation of sites, chain initiation by monomer, chain propagation, chain transfer to hydrogen, and spontaneous and by hydrogen deactivations. The equations of these reactions are presented in Table 1, where C_p denotes a potential site, P_{δ}^k a site of type k , $P_{\delta,i}^k$ a initiated chain with monomer type i and site type k , $P_{n,i}^k$ a live polymer chain with n monomers with end group i and active site k , M_i a monomer molecule of type i , C_d a dead site and D_n^k a dead polymer chain with n monomers of site k .

Table 1: Reactions considered in the kinetic model.

Spontaneous site activation	$C_p \xrightarrow{k_{asp}^k} P_0^k$
Chain initiation by monomer i	$P_0^k + M_i \xrightarrow{k_{p0i}^k} P_{\delta,i}^k$
Chain propagation by monomer j	$P_{n,i}^k + M_j \xrightarrow{k_{pij}^k} P_{n+\delta,j}^k$
Chain transfer to hydrogen	$P_{n,i}^k + H_2 \xrightarrow{k_{ctH}^k} P_0^k + D_n^k$
Deactivation by hydrogen	$P_{n,i}^k + H_2 \xrightarrow{k_{dH}^k} C_d + D_n^k$ $P_0^k + H_2 \xrightarrow{k_{dH}^k} C_d$
Spontaneous chain deactivation	$P_{n,i}^k \xrightarrow{k_{dsp}^k} C_d + D_n^k$ $P_0^k \xrightarrow{k_{dsp}^k} C_d$

Mass balances for the main gases (ethylene, comonomers, solvent, and hydrogen) and polymeric species were used to obtain the gas phase and the polymer compositions. The momentum technique for the bulk polymer (the sum of live and dead polymer) was used to determine the molecular weight distribution. Empirical correlations previously adjusted with experimental data were used to obtain the melt index as a function of the weight average molecular weight predicted by the model.

A differential-algebraic equations (DAE) system arises when the kinetic model equations and the melt index empirical correlations are inserted in the mass balances. The resulting DAE system was solved using the integrator DASSLC¹ and the Matlab/Simulink² environment for input and output data manipulation. Each reactor model has 22 states and the simulation time was about 25 seconds for 11 days of plant data using a Pentium III with 800 MHz and 128 MB RAM.

The dataset A was then used to adjust some of model parameter to the studied process. A sensitivity analysis was carried out to select the key parameters to be adjusted. According to this analysis, the selected parameters to adjust yield and melt index were the pre-exponential coefficients and the activation energies of the following reactions: cross propagation, chain transfer to hydrogen, and hydrogen and spontaneous deactivation of active sites. The seven inputs of the model were: monomer, hydrogen and solvent concentrations, catalyst flow rate, height of the fluidized bed, reactor temperature, and total pressure. The dataset B was reserved to validate the model.

Figure 4 shows the comparison between the data set A for polymer yield rate values and the values predicted by the model. When comparing the model predictions with plant data, it becomes clear that the model dynamics must be improved for the second reactor. This could be achieved by including a term of tendency in the objective function.

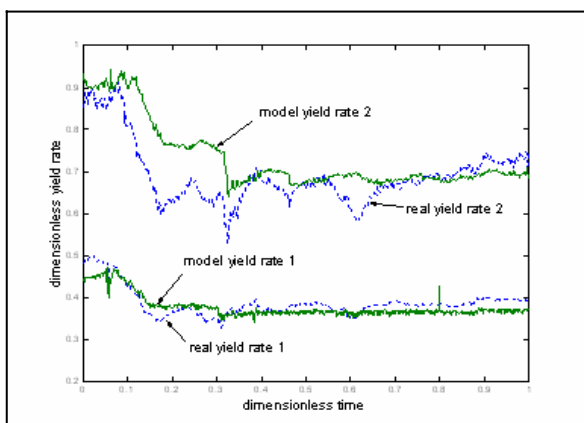


Figure 4: Plant data versus phenomenological model yield rate predictions for dataset A.

In Figure 5 the same comparison between plant data and model predicted values is presented for melt index. It can be noted that the model dynamics seems to be good, but a considerable offset can be observed.

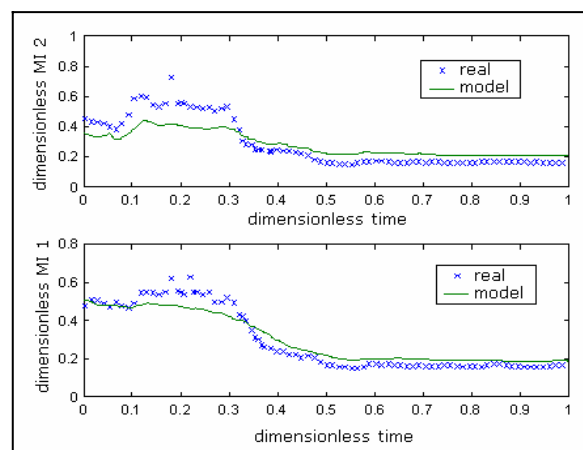


Figure 5: Plant data versus phenomenological model melt index predictions for dataset A.

The model validation will be presented in Section 4, where the phenomenological and the empirical models will be compared.

3. EMPIRICAL MODEL

For a given sample data, let the process input variables be collected as columns of an X matrix of rank r , whose rows represent different process observations. Let also the corresponding output variable values be collected as elements of a y vector. The dimension reduction methods perform the regression procedure in a subspace T extracted from the original X matrix. This subspace is constituted by at most r independent directions (latent structures or components), which are linear combinations of the original explanatory variables. The ability of building a model with the correct number of directions eliminates the collinearity problem and allows some noise filtration. The different dimension reduction methods are basically distinguished from one to another by the criteria considered to extract the latent structures from the original matrices. This work is focused in the linear and nonlinear PLS methods, which decompose the X matrix searching for the directions that better describe the response variable.

The linear PLS method proposed by Wold (1984) and its nonlinear extensions, Wold et al. (1989), Baffi et al. (1999), and Li et al. (2001), are based on the NIPALS (nonlinear iterative partial least squares) algorithm, which determines the subspace T where the regression is performed. Actually, the NIPALS algorithm extracts the latent structures t 's (T columns) from X one by one. Starting from the original X matrix, the algorithm determines the first weight vector w , extracts the direction $t = Xw$ and maps the y - t relationship using a general mapping function $\hat{y} = f(t)$. The direction t must provide the best fit according to the considered mapping function.

¹ <http://www.eng.ufrgs.br/enq/lib/numeric/numeric.html>

² Copyright The Mathworks, Inc.

The X matrix and the y vector are then orthogonalized with respect to t and \hat{y} . This procedure is then repeated using the orthogonalized X and y until the optimal number of extracted dimensions is achieved. Cross-validation tests or statistical criteria can be used to determine the optimal number of dimensions (Höskuldsson, 1996).

In this work two different versions of NIPALS algorithm were considered. The main difference between them is the applied mapping function. The algorithm proposed by Wold et al. (1984), the linear PLS method, is based on a linear mapping function $\hat{y} = bt$. Aiming to consider the existence of curvature in the X - y relationship, Wold et al. (1989) developed a nonlinear NIPALS algorithm that is based on a general mapping function f . In particular, the authors proposed the QPLS method, which employs a quadratic polynomial as mapping function: $\hat{y} = b_0 + b_1t + b_2t^2$. Afterwards, Baffi et al. (1999) suggested some modifications in the nonlinear NIPALS algorithm. Recently, Li et al. (2001) proposed the BTPLS method which resorts a highly flexible mapping function: $\hat{y} = b_0 + b_1 \cdot [\text{sgn}(t)]^{\delta} |t|^{\alpha}$.

In order to model the studied system input-output relationship, several stationary points were identified in the dynamics datasets A and B. These stationary points were used to estimate the steady-state gains for the melt index and polymer yield rate. Based on these steady-state gains and on known first and second order time constants of the process, empirical models were generated using PLS, QPLS and BTPLS methods in order to predict the system dynamics. The computations were carried out using the software Matlab³.

For PLS, QPLS and BTPLS methods, the melt index and yield rate variability explained by each component ($j = 1, 2, \dots, 7$) is presented in Table 2 for both reactors. The significance of the increase that each component causes in the cumulative explained variance was tested by a standard t -test. In Table 2, the significant and the insignificant components are respectively presented in bold and grey numbers. The insignificant components were neglected to avoid overfitting.

As it can be noted, QPLS and BTPLS exhibit higher capacity in explaining the output variables variability. For both reactors, the single significant component of both nonlinear methods is able to explain more than 95% of melt index and yield rate.

Once it could not be observed considerable difference in fitting performance between the nonlinear methods, QPLS was chosen to be compared with the phenomenological model because it is expected to provide more reliable predictions when the original model space is extrapolated.

Table 2: PLS modelling summary.

	j	PLS	QPLS	DTPLS	PLS	QPLS	DTPLS
		Cumulative Melt Index Explained Variability (%)			Cumulative Yield Rate Explained Variability (%)		
REACTOR 1	1	93,53	97,10	96,97	81,01	99,90	95,82
	2	96,97	97,33	98,68	84,08	97,33	97,68
	3	96,29	99,00	97,62	00,00	99,40	99,02
	4	96,17	99,76	97,76	92,36	98,61	98,38
	5	96,67	99,53	97,78	93,43	98,73	98,67
	6	96,70	99,35	97,62	94,76	98,34	98,68
	7	96,00	99,73	97,52	96,61	99,37	99,76
REACTOR 2	1	94,16	97,45	90,09	73,30	97,10	97,14
	2	89,12	97,33	99,01	92,58	98,13	97,36
	3	97,10	98,33	99,07	95,34	98,32	97,65
	4	97,79	99,45	99,11	96,72	99,70	99,09
	5	98,86	99,53	99,11	97,09	98,31	98,11
	6	98,82	99,35	99,16	97,10	98,32	98,19
	7	98,82	99,73	99,16	97,11	98,33	98,26

4. COMPARISON BETWEEN MODELS

In order to compare the phenomenological and empirical methodologies, the previously generated phenomenological and QPLS models were used to predict the transient behaviour of data set B. The results are reported in Figure 6, Figure 7, Figure 8, and Figure 9.

When the phenomenological and QPLS predictions for polymer yield rate are compared, it becomes clear that the empirical model have superior capability in describing the process dynamics. The empirical model also exhibits a considerably smaller bias. The analysis of the melt index predictions is presented in Figure 8 and Figure 9. Again, the QPLS method exhibited outstanding predictive performance.

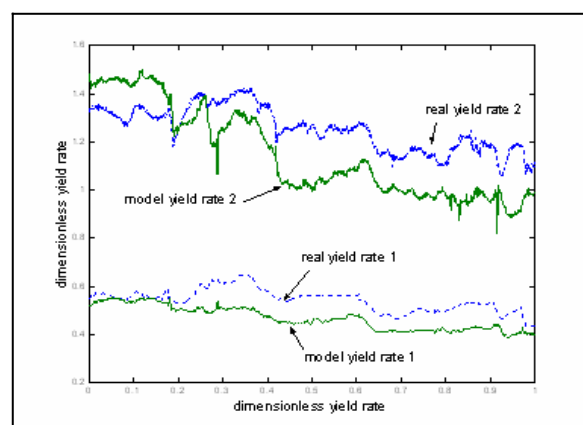


Figure 6: Plant data versus phenomenological model yield rate predictions for dataset B (validation).

³ Copyright The Mathworks, Inc.

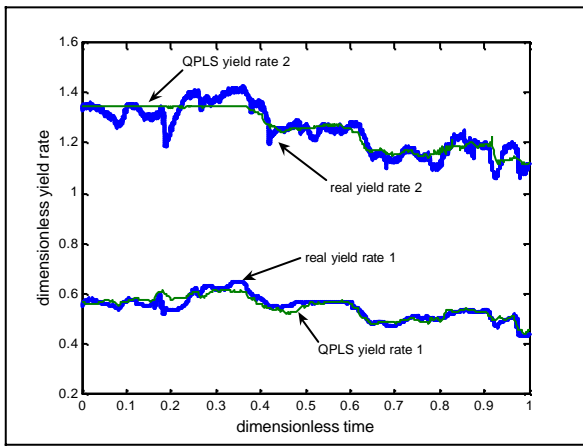


Figure 7: Plant data versus one-component QPLS model yield rate predictions for dataset B (validation).

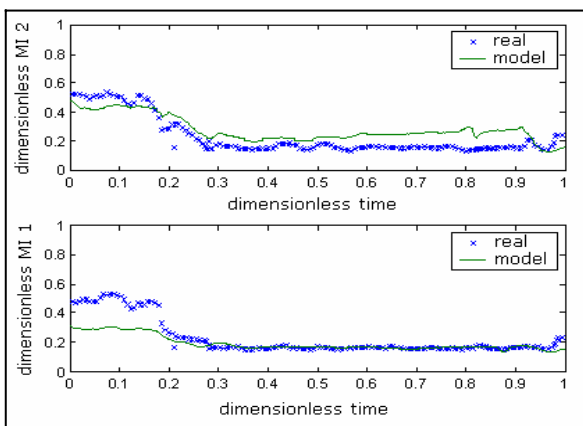


Figure 8: Plant data versus phenomenological model melt index predictions for dataset B (validation).

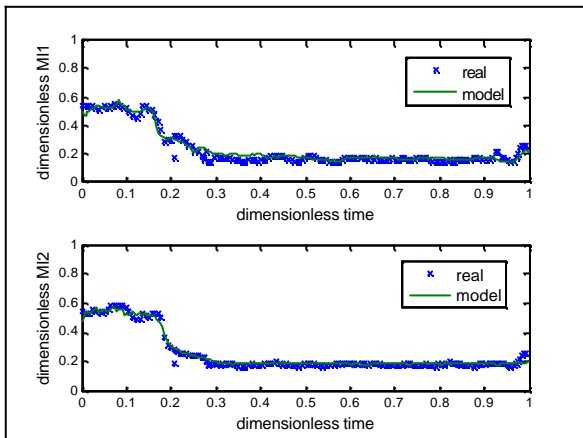


Figure 9: Plant data versus one-component QPLS model melt index predictions for dataset B (validation).

5. INDUSTRIAL APPLICATION

To illustrate the applicability of the developed models, the QPLS model for the melt index was used as virtual analyzer of a predictive controller (MPC) for the MI. Figure 10 and Figure 11 show historical data of MI in opened and closed loop. The MI data in

these figures correspond to measurements performed in laboratory from samples taken at each two hours.

The virtual analyzer used in the closed loop provides predicted values of MI to the controller at time intervals of one minute, improving the controller action and the polymer quality, as observed in Figure 11 where the dashed line at normalized MI = 1 is the setpoint.

As can be observed in Figure 12, which shows the normal distribution curves built with the means and standard deviations of opened and closed loop data, the melt index variability was significantly reduced by the controller.

It is important to observe that the dashed lines at normalized MI equal to 0.8 and 1.2 in Figure 11 and Figure 12 correspond to the lower and upper MI specification limits. Consequently, these figures indicate that the closed loop strategy reduced the out of specification products. These results are confirmed by evaluating the process capability index (CPK), defined as the ratio between permissible deviation, measured from the mean value to the nearest specific limit of acceptability and the actual one-sided 3σ spread of the process, Montgomery (1991), and taking into account that larger values of CPK mean higher product quality. The CPK for the opened loop was 0.40 and for the closed loop was 1.00.

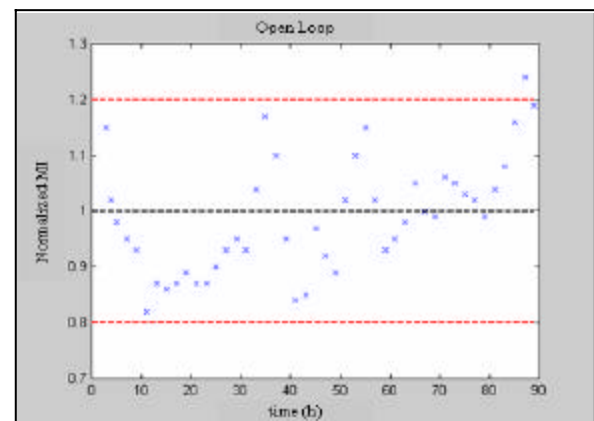


Figure 10: Historical melt index opened loop data.

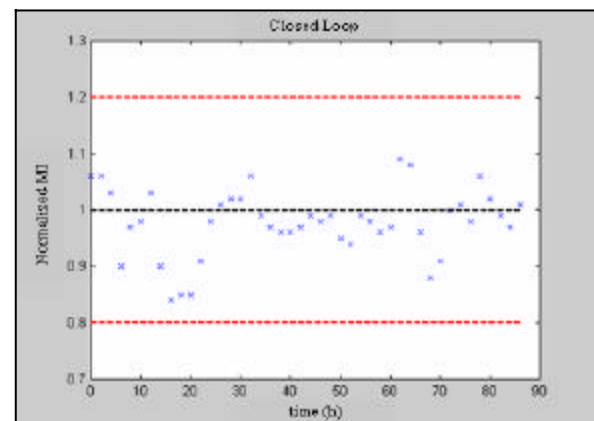


Figure 11: Historical melt index closed loop data.

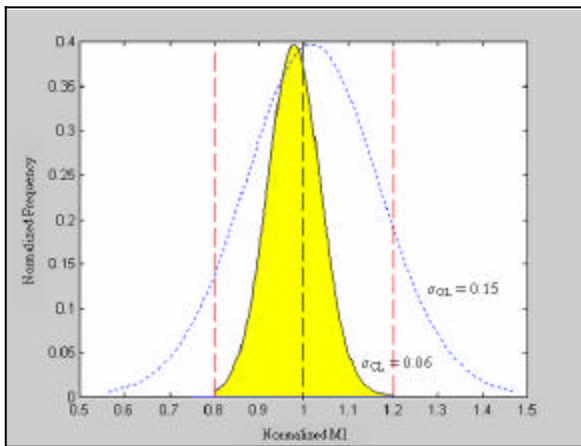


Figure 12: Distribution curves for the open loop and the closed loop.

6. CONCLUSION

Models of different types for ethylene polymerization reactors were adjusted with process industrial data. The comparison between these models showed better results for the empirical models with nonlinear steady-state gains and linear dynamics.

The empirical model for the melt index was successfully used as virtual analyzer of an advanced control strategy for an industrial plant, improving the controller action and the polymer quality by reducing significantly the process variability.

REFERENCES

- Baffi, G., Martin, E.B and Morris, A.J. (1999), Non-Linear projection to latent structures revisited: the quadratic PLS algorithm, *Computers and Chemical Engineering*, **23**, 395.
- Bindlish, R., Rawlings, J.B. and Young, R.E. (2003), Parameter Estimation for Industrial Polymerization Processes, *AIChE J.*, **49**(8), 2071.
- Choi, K.Y. and Ray, W.H. (1985), The Dynamic Behaviour of Fluidized Bed Reactors for Solid Catalyzed Gas-Phase Olefin Polymerization, *Chem. Eng. Sci.*, **40**, 2261.
- Finkler, T.F. (2003), *Desenvolvimento de uma Ferramenta para Obtenção de Modelos Empíricos*, Master Thesis, Universidade Federal do Rio Grande do Sul, Porto Alegre, 2003.
- Gambetta R., Zacca J.J. and Secchi A.R. (2001) Model for Estimation of Kinetics Parameters in Gas-Phase Polymerization Reactors. *In proceedings of the 3rd Mercosur Congress on Process Systems Engineering* Santa Fé, Argentina, vol. II, 901-906.
- Höskuldsson, A. (1996), *Prediction Methods in Science and Technology*, Thor Publishing, v.1, 1996.
- Kunii, D. and Levenspiel, O. (1991), *Fluidization Engineering*, 2nd Edition, Butterworth-Heinemann, New York.
- Li, B., Martin, E.B and Morris, A.J. (2001), Box-Tidwell based partial least squares regression, *Computers & Chemical Engineering*, **25**, 1219.
- McAuley, K.B. and MacGregor, J.F. (1991), On-line inference of polymer properties in an industrial polyethylene reactor, *AIChE J.*, **37**(6), 825.
- Montgomery, D. (1991), *Introduction to Statistical Quality Control*, John Wiley & Sons, New York
- Sato, C., Ohtani, T. and Nishitani (2000), H., Modeling, simulation and nonlinear control of a gas-phase polymerization process, *Comp. Chem. Eng.*, **24**, 945.
- Soroush, M. (1998), State and parameter estimations and their applications in process control, *Comp. Chem. Eng.*, **23**, 229.
- Wold, S. Ruhe A., Kettaneh N. and Skagerberg B. (1989), Nonlinear PLS modeling, *Chemometrics and intelligent laboratory systems*, **7**, 53.
- Wold, S. Ruhe A. and Wold H. (1984), Dunn, W.J., The Collinearity Problem in Linear Regression: The Partial Least Squares Approach to Generalized Inverses, *Siam J. Sci. Stat. Comput.*, **5**, 735.
- Zhao, H., Guiver, J., Neelakantan, R. and Biegler, L.T. (2001), A nonlinear industrial model predictive controller using integrated PLS and neural net state-space model, *Control Eng. Practice*, **9**, 125.